Defence Science Journal, Vol. 66, No. 6, November 2016, pp. 638-644, DOI : 10.14429/dsj.66.9659

Effect of Rotor Blade Geometry on the Performance of Rotary-Winged Micro Air Vehicle

Kirti Bhatnagar and Abhishek*

Department of Aerospace Engineering, IIT Kanpur, Kanpur - 208 016, India
**E-mail: abhish@iitk.ac.in*

ABSTRACT

The development of physics based analysis to predict the hover performance of a micro rotor system meant for a hover capable micro air vehicle for studying the role of blade geometric parameters (such as planform, twist etc.) is discussed. The analysis is developed using blade element theory using lookup table for the sectional airfoil properties taken from literature. The rotor induced inflow is obtained using blade element momentum theory. The use of taper seems beneficial in improving the hover efficiency for lower values of thrust coefficient. For rotors operating at high thrust conditions, high negative twist is desirable. There is no unique blade geometry which performs well under all thrust conditions. This well validated analysis can be used for design of hover capable micro air vehicles.

Keywords: Micro air vehicles, Low Reynold's number, aerodynamic performance, micro rotor

1. INTRODUCTION

Recent years have witnessed an exponential growth in interest / activities related to a new class of flight vehicle called micro air vehicle (MAV), which has a great potential for wide-ranging applications. Depending on the mission profile, such a vehicle can carry a useful payload which would typically be an assortment of sensors, for example, optical, chemical, radiological, and/or radio transmitter. The mission profile envisioned for such vehicles includes eye-in-the-sky robot, that would be carried and operated by an individual or in an autonomous manner with minimal human intervention, for increased situational awareness while minimising his/her risk. Increased interest in the MAVs can be seen as the direct outcome of the recent advances in electronic surveillance and detection equipment which allow them to be miniaturised to fit them within tens of grams[1].

The current generation of MAV includes fixed wing, flapping wing and rotary wing vehicle. Fixed wing vehicles are well suited for outdoor reconnaissance missions that do not require hovering at a location or manoeuvering in tightly constrained spaces. However, for missions around or within buildings hovering vehicles have a clear advantage over fixed wings configurations due to their low speeds**.** The possibility of using ideas such as tail sitter fixed wing airplanes which can transition into hovering mode was explored in Autonomous Hovering of a fixed wing micro air vehicle[2]**.** But, these vehicles suffer from poor control authority for manoeuvering at low speeds and also have poor hovering efficiency. Ideally, a stealthy hovering MAV can fly indoors without being detected and can potentially have the ability to 'perch and stare', providing tactical reconnaissance and surveillance for extended periods of time with low risk of detection.

Two different MAV configurations are capable of hovering flight: flapping wing (insect like) and rotary wing vehicles. The potential for high efficiency in flapping-wing configurations has been demonstrated for aircraft of the MAV-size and smaller[3-5],but the mechanical and aero elastic complexity of such mechanisms are hurdles that remain to be overcome. The simplicity of rotary wing vehicle design when compared to its flapping wing counterpart, combined with lower noise levels and greater stability make it an attractive candidate for MAV applications[6-8].

MAVs due to their size, operate at low Reynolds number. Therefore, the airfoil operating at low Reynolds number experiences many complex flow phenomena within the boundary layer and MAV development faces many unique challenges that make their design and development difficult[9].As a result of low Reynolds number, hovering performance of micro rotor based vehicles is poor compared to a full scale vehicle. A typical battery powered micro helicopter has a maximum hover endurance of 15 min. Apart from low power density of the Lithium-Polymer batteries, poor hover performance is also due to low aerodynamic efficiency of micro rotors which is a result of high profile power. Felipe[6,7] studied the performance of the micro rotors in single as well as coaxial configurations in great detail**.** He conducted experiments to systematically measure the performance of various rotor geometries and then developed theory for its prediction. In order to improve the hover performance, shrouded rotors have been used which offer higher power loading in hover, but are more susceptible

Received : 22 January 2016, Revised : 12 May 2016
Accepted : 07 June 2016, Online published : 25 October 2016

to oscillations when exposed to external flow disturbances when compared to an unshrouded rotor[10]. Felipe[6,7] and Singh & Venkatesan[11], carried out micro rotors test in single and coaxial configurations for different rotor geometries. Since, the rotor aerodynamic power was measured indirectly by measuring the electric power consumed by the electric brushed DC motors, instead of the mechanical power being transmitted to the shaft, the experimental data is less useful for validation of theoretical aerodynamic power calculations.

Since, the rotor blade airfoil section has significant influence on the hover efficiency of the rotor, a series of rotor parameters that affect the performance of the rotor were studied by Hein and Chopra[12]. In this study, it was concluded that a blade with circular arc cambered airfoil provided significant improvement in hover efficiency compared to conventional thick airfoils and flat plate airfoils. A systematic experimental study investigating the effect of rotor parameters such as blade airfoil, blade chord, blade twist, and planform taper, on the performance measurements was carried out by Benedict[13], *et al.* In this study airfoils operating at Reynolds number as low as 30,000 were experimentally tested and based on the understanding of the impact of various parameters an optimum rotor design for MAVs was created, which produced a figure of merit of 0.67, which is the highest value of Figure of Merit ever reported in the literature for micro-rotors. It was also concluded that the hover efficiency increases with blade chord for thin cambered plate airfoils at high solidity, with insignificant effect of twist on the performance. To help understand the various aerodynamic losses on a micro-rotor at low tip Reynolds number, Digital particle image velocimetry (DPIV) measurements were performed by Ramasamy[14], *et al.* to interrogate the flow field near the micro rotors and obtain insight into the span wise loads and overall aerodynamic performance of micro rotor system. It was concluded that blades with sharpened leading edge performed better than those with blunt leading edge by consuming less power for same thrust or by generating higher thrust for same power consumption**.** Recently, efforts have been undertaken for studying the feasibility of using micro rotors for exploration of other planetary environments such as that of Mars[15]. A regular micro rotor operating on Mars would experience flow-field at extremely low Reynolds number, even lower than 5000. The study demonstrated the feasibility of using a coaxial rotor MAV on Mars with a realistic endurance of up to 13 min but the rotors could only achieve a maximum figure of merit of 0.4.

The aim of this study is to develop physics based analysis to predict the hover performance of a micro rotor system and study the role of blade geometric parameters (such as planform, twist etc.). Such an analysis can be used for performance study and design of micro rotor systems. The analysis is developed using blade element theory (BET)[16], in which sectional airfoil properties are obtained using airfoil table lookup and the inflow is obtained using blade element momentum theory. Airfoil tables for 6 per cent camber circular arc airfoils are taken from Felipe[6] which is generated using CFD computations. Circular arc airfoils are commonly used in rotary winged MAVs and hence are used for the present analysis. Since the comprehensive airfoil data is available only for 6 per cent cambered airfoil, only the rotor geometric parameters are changed in the present analysis. The inflow equation obtained using BEMT is solved using a non-linear equation solver to get non-uniform inflow distribution in hover.

2. APPROACH AND METHODOLOGY

The analysis of micro helicopter rotors is dominated by the complex aerodynamics surrounding the rotor. The flexibility, usability and accuracy of blade element momentum theory (BEMT) make it suitable for performance prediction for hovering flight condition. The BEMT is a mathematical model that combines the basic principles from both blade element and momentum theory approaches to estimate the non-uniform inflow distribution along the blade. Due to the low Reynolds number (15000 – 60000), rotor based MAVs use circular arc airfoils for their blades. Therefore, this research focuses on improving the performance of these blades. A typical blade used on rotor based MAVs is shown in Fig. 1.

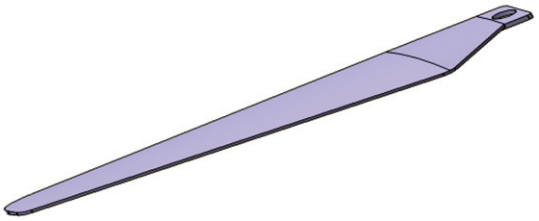

Figure 1. Circular arc airfoil based micro rotor blade.

2.1 Blade Element Momentum Theory

The rotor disc area can be discretised in to concentric annuli of radius and area $dA = 2\pi ydy$ as shown in Fig. 2. Applying one-dimensional momentum theory to a rotor in axial hovering flight, the thrust produced by each annulus is given by:

$$dT = 2\rho v_i^2 dA = 4\pi\rho v_i^2 ydy \quad (1)$$

where ρ density of air is, v_i is induced velocity of the rotor. The non-dimensional thrust coefficient is then given by:

$$dC_T = 2\rho v_i^2 dA / \rho\pi R^2 (\Omega R)^2 \quad (2)$$

where C_T is the thrust coefficient, R is the radius of the rotor and Ω is the rotational speed of the rotor. Detailed discussion of the above theory is available in Leishman[16].

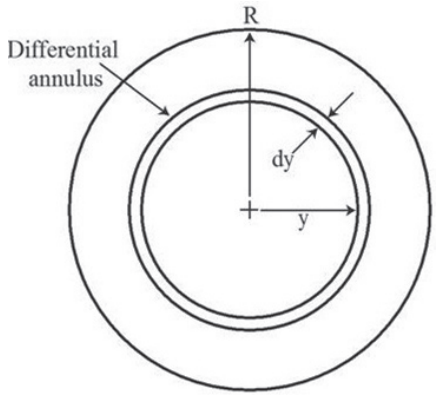

Figure 2. Annulus of Rotor disc for BEMT analysis.

In the non-dimensional form the above equation is:

$$dC_T = 4\lambda^2 r dr \tag{3}$$

where λ is inflow through the rotor. The incremental thrust coefficient of the annulus from blade element theory is:

$$dC_T = \sigma C_l r^2 dr / 2 \tag{4}$$

where $\sigma\left(= N_b c / \pi r\right)$ is the rotor solidity defined as ratio of blade area to rotor disc area and C_l is the local lift coefficient. For hovering condition inflow in climb, $\lambda_c = 0$. Now combining the blade element (Eq.4) and momentum theories (Eqn 3) we can obtain new equation in λ:

$$\sigma C_l r^2 dr / 2 = 4\lambda^2 r dr \tag{5}$$

The resulting equation is a non-linear equation in inflow. Non-linearity should be noted that C_l is a function of angle of attack α and Reynolds number. After the inflow is determined, the incremental thrust of each blade element is obtained using

$$dC_T = \frac{1}{2}\alpha C_{l_\alpha}\left(\theta r^2 - \lambda r\right)dr \tag{6}$$

where θ is collective pitch angle and r is radial station along the blade.

The total thrust, induced power coefficient, C_{P_i}, and profile power coefficient, C_{P_0} are calculated by numerically integrating over the blade.

$$C_{P_i} = \int_{r=0}^{r=1} \lambda dC_T \tag{7}$$

$$C_{P_0} = \frac{1}{2}\sigma \int_{r=0}^{r=1} C_d r^3 dr \tag{8}$$

2.2 Prandtl Tip Loss Function

The preceding equations are modeling the viscous losses through airfoil's drag coefficient, and part of induced losses by calculating a non-uniform inflow distribution. The loss of lift near the tips resulting from the induced effects associated with a finite number of blades. Prandtl provided a solution to the problem of loss of lift by including a correction factor F:

$$F = \left(\frac{2}{\pi}\right)\cos^{-1}\left(\exp\left(-f\right)\right) \tag{9}$$

where f is given in terms of no. of blades, N_b and radial position of blade: $f = N_b\left(1-r\right)/2\left(r\phi\right)$ and ϕ is induced inflow angle $\left(=\lambda\left(r\right)/r\right)$.

Prandtl's F function increases the induced velocity at the tip and reduces the lift generated there. For hovering flight Eqn 3 is modified by using Prandtl's tip loss factor:

$$dC_T = 4F\lambda^2 r dr \tag{10}$$

Expression of inflow can be derived as:

$$\lambda\left(r\right) = \left[\sqrt{1+\frac{32F\theta r}{\sigma C_{l_\alpha}}} - 1\right]\sigma C_{l_\alpha} / 16F \tag{11}$$

where C_{l_α} is lift curve slope and σ is solidity of the rotor.

As F is a function of λ in Eqn. (11), the above equation need to be solved iteratively. An initial value of F equal to 1 is assumed and the resultant λ is used in Eqn. (11) to recalculate F. The process is repeated until the convergence is achieved.

Since, the tip loss factor is nearly 1 for 75 per cent of blade span and becomes zero near the blade tip, inflow tends to infinity towards the tip region as shown in Fig. 3(a). Figure 3(b) shows the distribution of thrust over the blade span with tip loss and without tip loss. Figure 3 shows the influence of tip loss near 70 per cent of the span because the formation of a trailed vortex at the tip of each blade produces a high inflow over the tip region and effectively reduces the lifting capability there. The performance parameters for hovering flight are initially calculated using fixed values of drag coefficient $(C_{d_0} = 0.01)$ and lift coefficient $C_{l_\alpha} = 2\pi$. The use of constant lift curve slope and drag coefficient produces inaccurate thrust and power predictions for micro rotors. Therefore, lift and drag data for different Re (15,000 to 60,000) available in Felipe[6] for 6 per cent camber airfoil is used to calculate sectional lift and drag through table look-up. In table look-up scheme, the lift curve slope and drag coefficient corresponding to the calculated angle of attack and Reynolds number are interpolated using the available data. The numerical integration of various performance parameters over the entire blade is obtained by using six point Gaussian quadrature.

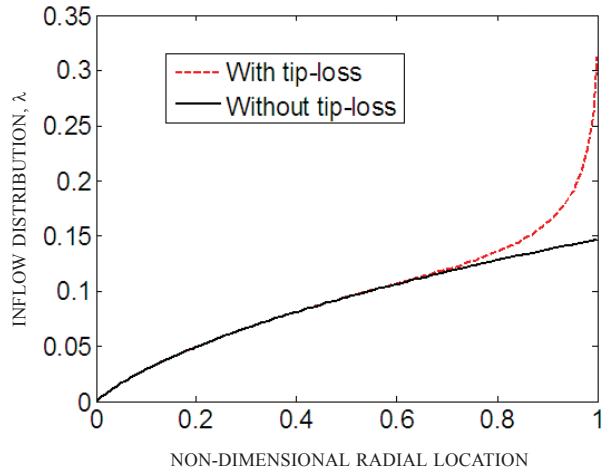

(a)

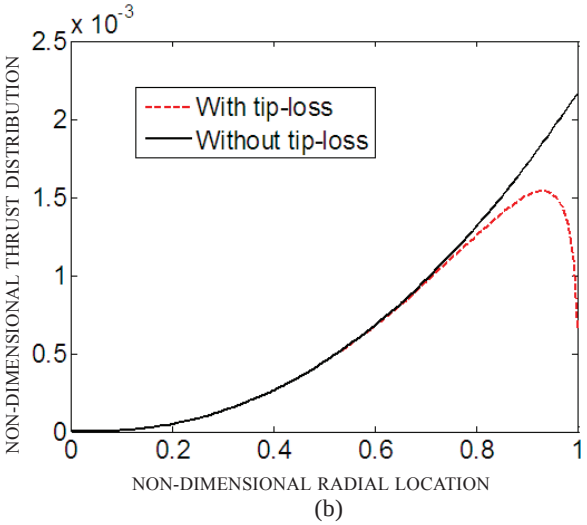

(b)

Figure 3. Effect of Prandtl tip loss factor on inflow calculation and thrust distribution for same pitch angle: (a) Inflow distribution and (b) Thrust distribution.

2.3 Iterative Calculation of Performance Parameters

Since the inflow has to be calculated using a non-linear solver the initial guess values of inflow have to be obtained. Therefore, the calculation is initiated by using closed form equations of inflow based on constant lift curve slope of 2π. Since, the lift and drag data for conventional airfoils is not valid for circular arc airfoils operating at low Reynolds number, lift and drag data for different Re (15,000 to 60,000) available in literature is used for performance predictions. It should be noted that this data was generated using CFD analysis. The integration of the various performance parameters over the entire blade is carried out by dividing the rotor in 20 equal sized segments and then using six point Gaussian quadrature over each segment.

3. RESULTS

Before studying the effect of blade parameters on the performance, the current analysis is validated against the experimental and analytical results available in literature.

For the rotor configuration given in Table 1, the performance prediction is carried out by varying the collective pitch angle from 0 to 18 in steps of 2°. In addition to study the prediction capability at different rpms rotational speed is varied from 2500 rpm to 5000 rpm in steps of 500 rpm. Figure 4 compares the non-dimensional power *vs* non-dimensional thrust predicted by present analysis at 2500 rpm for above rotor with existing experimental data and another BEMT based calculation taken from Felipe[6]. The prediction shows good correlation with the experimental results. Figure 5 shows the comparison for C_T vs. Figure of Merit (FM) which shows good correlation with experimental data for moderate values of C_T. The drop in Figure of Merit at high values of C_T is due to the blade stall as the blade is operating at high pitch angle. The over prediction of FM by current analysis may be attributed to the inaccuracies in the prediction of static stall for the circular arc airfoil at low Re by the commercial CFD code.

Table 1. Baseline blade parameters (all dimensions in m)

Parameters	Dimentions (m)
Rotor radius	0.1120
Blade chord	0.0225
Solidity	0.1279
Number of blades	2
Blade planform	Rectangular
Camber	6 per cent

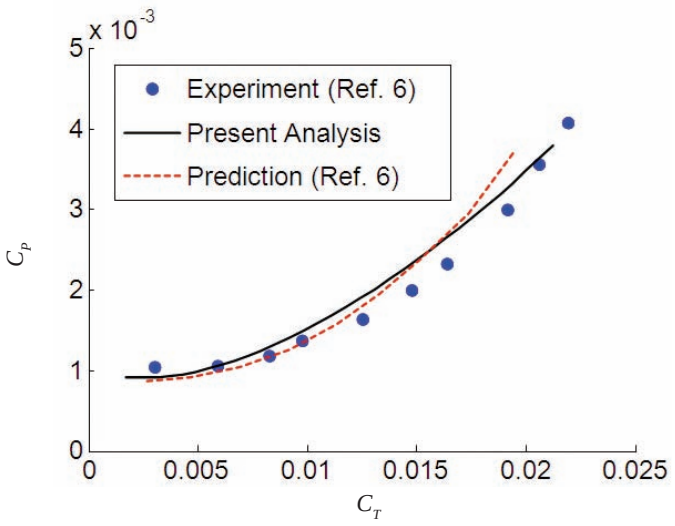

Figure 4. Experimental and predicted C_P vs. C_T for baseline blades at 2500 rpm.

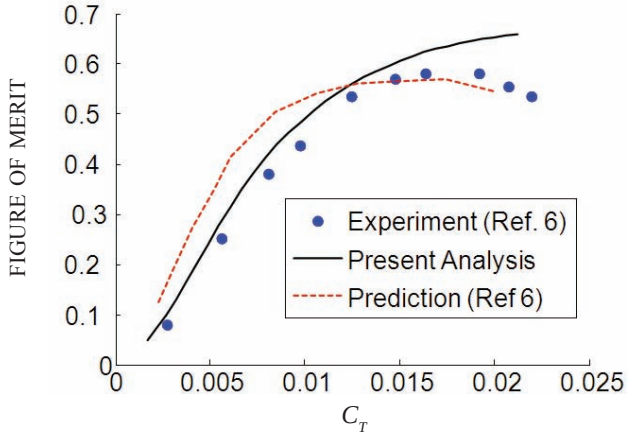

Figure 5. Experimental and measured Figure of Merit vs. C_T for baseline blades at 2500 rpm.

The role played by low Re on the performance prediction can be understood from Fig. 6, which shows the comparison of predicted thrust vs. pitch angle with experimental results for different rpm. The increase of rpm from 2500 to 5000 changes the tip Re from 4.7×10^4 to 9.5×10^4 . The predictions show better correlation with increasing rpm (Fig. 6) which is due to more accurate calculation of sectional airfoil characteristics using CFD at higher Re. In general the analysis is able to predict the performance well at all rpms. It should be noted that rotary wing MAVs typically operate at or around 3500 rpm.

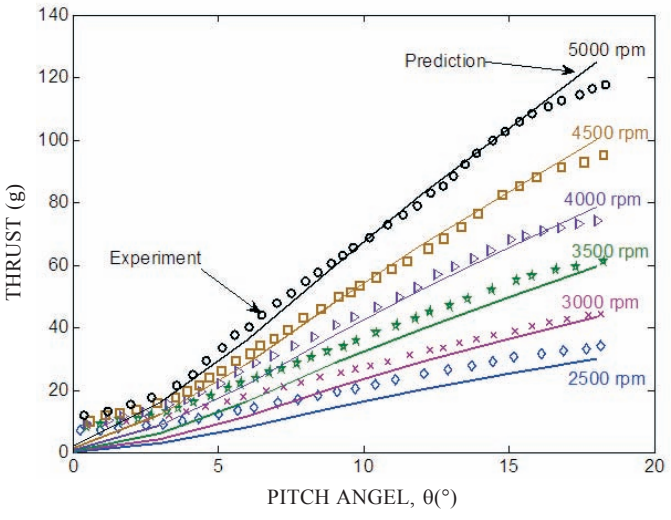

Figure 6. Comparison between experiment and prediction at various rotational speeds.

3.1 Fundamental Understanding

The role of geometric parameters of blade at low Re is systematically studied by comparing the change in performance over the baseline rectangular rotor blades. Effect of geometric parameters such as chord, radius, taper and twist is discussed in coming sub-sections.

3.1.1 Effect of Chord

Performance of 6 per cent cambered circular arc blades of different chord lengths is compared. All other geometric parameters are kept constant. The baseline chord selected for the present analysis is 22.5 mm. The results comparing the C_P *vs.* C_T for four different chord lengths are shown in Fig. 7. It is observed that the effect of increasing chord is to increase power consumption for same thrust output; this is due to increase in profile power which increases with chord for lower values of C_T as shown in Fig. 8(a). This effect becomes less pronounced with increasing collective as blades with different chords consume same power at given C_T. This is due to the fact that at higher C_T, the induced power is the dominant component of the total power which remains unaffected by change in chord as shown in Fig. 8(b). Induced power only depends on the amount of thrust generated and therefore is independent of blade geometry change (note that change in Re due to chord change is negligible). Smaller chord value seems to be more desirable. However, chord cannot be reduced beyond a limit to maintain structural rigidity of the blades and to prevent the blades from operating close to stall for high thrust cases.

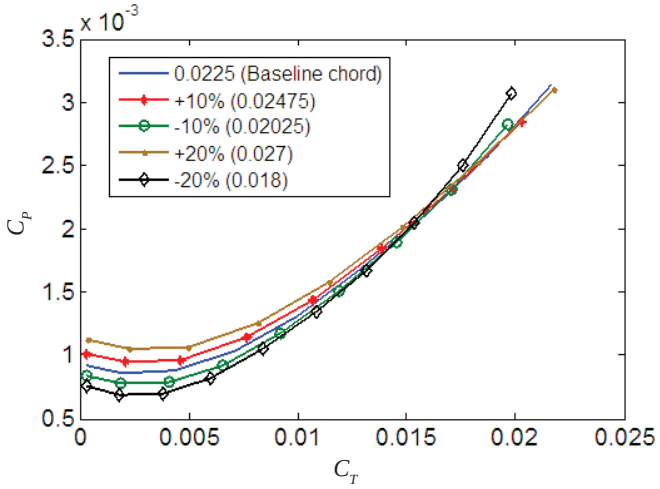

Figure 7. C_p *vs.* C_T for various chord lengths.

3.1.2 Effect of Radius

The Baseline radius of the rotor for the present analysis is 117.9 mm. The performance analysis is carried out at ±10 per cent and ±20 per cent variation of the baseline radius. The results are shown in Fig. 9 and are similar to that observed for the chord variation. The power consumption increases with decrease in rotor radius for same thrust**,** which is again due to the variation of profile power. Induced power again remains unaffected from rotor geometry change and is not shown. Profile power (Fig. 10) increases with decrease in rotor radius due to increase in rotor solidity. The difference in power consumption at higher values of thrust coefficient is less due to the increase in drag

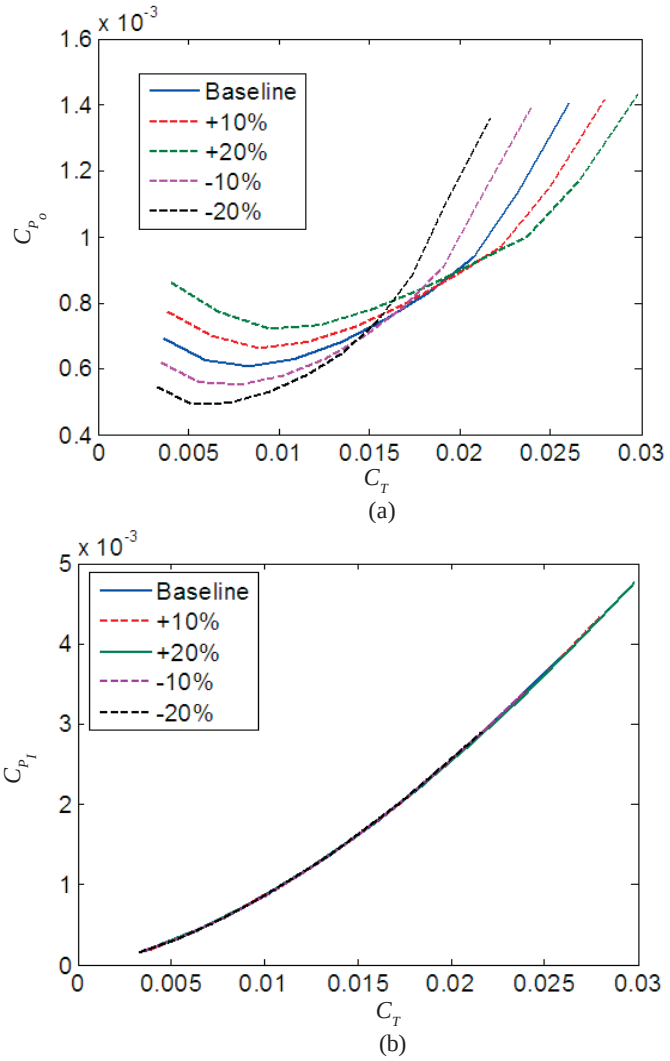

Figure 8. Induced power and profile power coefficients vs thrust coefficient at 2500 rpm : (a) Profile power *vs.* thrust (b) Induced power *vs.* thrust.

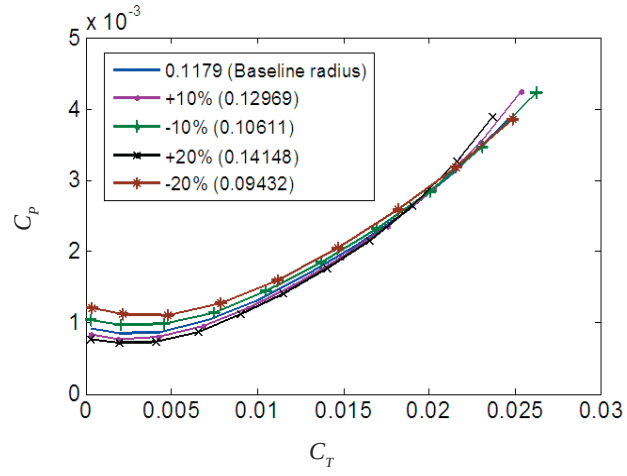

Figure 9. C_P *vs.* C_T at different values of rotor radius.

coefficient which possibly overcomes the effect of increased rotor solidity. In general, larger radius appears to be a better choice for improving the performance.

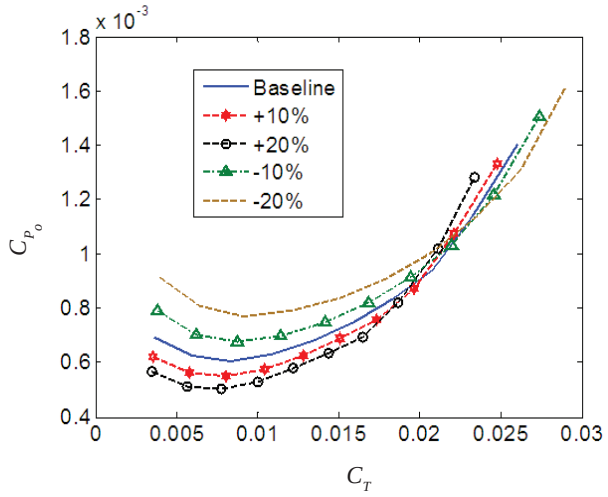

Figure 10. Comparison of profile and induced power coefficients with pitch angle at 2500 rpm.

3.1.3 *Effect of Taper*

Taper in blade planform is desirable to make blade sections operate close to their local maximum lift-to-drag ratio to minimise profile power consumption. As taper ratio is increased, figure of merit is expected to improve**,** which is indicative of improved hover performance**.** The comparison of figure of merit vs. C_T for three asymmetric taper ratios (2:1, 1.66:1 and 1.33:1) and the baseline blades at 4000 rpm is shown in Fig. 11. Up to a C_T of 0.015, the use of taper seems to be improving figure of merit, but at higher values of C_T the untapered blade shows higher value of figure of merit than the tapered blades. This is due to the fact that, the presence of taper decreases local lift and therefore to generate same amount of thrust the blade has to operate at higher values of blade pitch angle, resulting in higher angle of attack. Therefore taper blades although being more efficient, stall earlier than the untapered blades resulting in a drop in figure of merit at high thrust conditions.

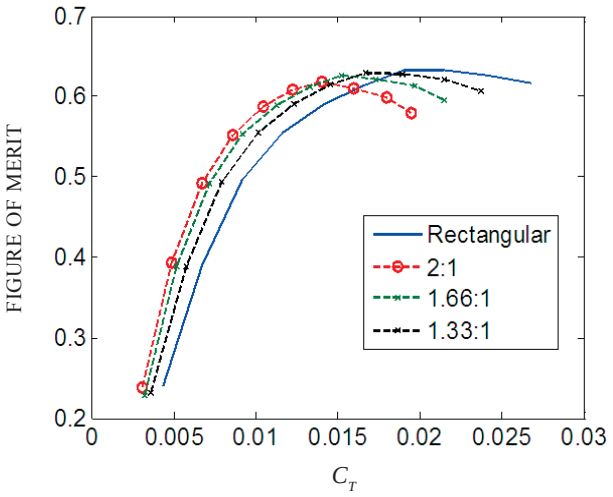

Figure 11. C_P vs. C_T for various asymmetric taper ratios at 4000 rpm.

3.1.4 *Effect of Twist*

The induced power component of a hovering rotor is at a minimum when the inflow distribution across the blade is uniform. This is achieved by introducing a significant negative twist in the blades. Thus, twist is a key ingredient in improving figure of merit of a rotor by reducing induced power consumption. Therefore, the baseline rotor performance is compared with three different rate of twist: +5°, -10° and -20°. The results are shown in Fig. 12. Unlike full scale helicopters the effect of twist on rotor performance is less significant. Lower power consumption for twisted rotor is only observed for higher values of C_T. The diminished role of twist may be attributed to larger magnitude of profile power compared to induced power at lower C_T conditions, as a result of which decrease in induced power has less impact on total power. This situation is primarily due to increased viscous losses at low Reynolds number.

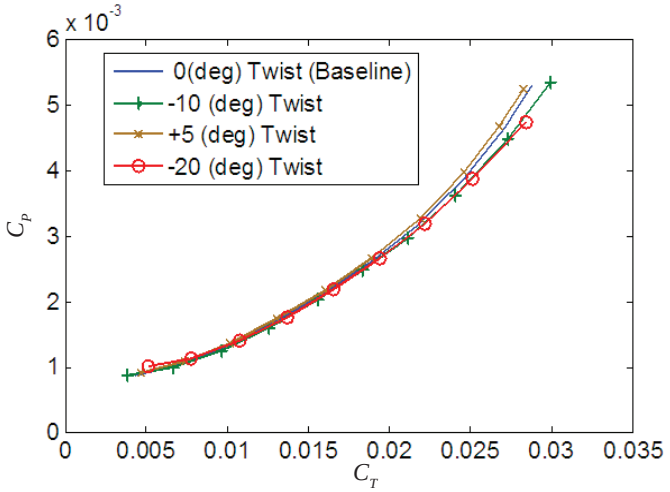

Figure 12. C_P vs. C_T for different values of twist at 2500 rpm.

4. CONCLUSIONS

A blade element momentum theory based analysis is developed to predict the performance of micro rotor blades used in rotary wing MAVs. Blade aerodynamic properties for a circular arc airfoil are taken from literature. The analysis is validated using available experimental data. Based on this research work the following conclusions can be made:

(i) In general, using a blade with high aspect ratio (lower chord or larger radius) is beneficial in reducing the profile power consumption. Based on present analysis, increasing the blade radius is recommended over decreasing the chord.

(ii) Using 2:1 taper improves the figure of merit for lower value of C_T, but at higher value of C_T the advantage of using taper is negated due to blade stall. Therefore, to extract maximum benefits from the use of taper an airfoil with better stall characteristics than the 6 per cent camber needs to be selected. It should be noted that in the present analysis, the effect of variable chord on the percentage camber of the airfoil section has not been considered. To model this effect, additional airfoil tables corresponding to different camber would have to be obtained.

(iii) Twist does not have any significant effect on power consumption at low C_T values, but for rotors operating at high C_T values, use of twist may be beneficial in reducing power consumption.

(iv) There is no 'silver bullet' parameter which can be used to help enhance rotor performance for all operating conditions. Therefore, a more careful optimisation needs to be carried out to truly exploit the effect of various geometry parameters.

(v) The present analysis is able to predict the performance of rotor thrust and power for micro rotors with good accuracy and hence can be used for design and sizing of MAV rotors of various configurations.

REFERENCES

1. Mueller, T. & De Laurier, J. Aerodynamics of Small Vehicles. *Annual Rev. Fluid Mech.*, 2003, **35**, 89-111.
2. William, E.G. & Paul, Y. oh. Autonomous hovering of a fixed wing micro air vehicle. *In* Proceedings of the 2006 IEEE International Conference on Robotics and Automation, Orlando, Florida, May 2006.
3. Singh, B. Dynamics and aero elasticity of hover capable flapping wings: Experiments and analysis. Department of Aerospace Engineering, University of Maryland, College Park, 2006. (PhD thesis).
4. Seshadri, P.; Benedict, M. & Chopra, I. Experimental investigation of an insect-based flapping wing hovering micro air vehicle. Presented at the Aeromechanics Conference of the American Helicopter Society, Jan 20-22, San Francisco, 2010.
5. Bhowmik, J. Design, Development and aerodynamic analysis of an efficient flapping wing flying vehicle. Department of Aerospace Engineering, IIT Kanpur, Kanpur, 2012. (MTech thesis).
6. Bohorquez, F. Rotor hover performance and system design of an efficient coaxial rotary wing micro air vehicle. Department of Aerospace Engineering, University of Maryland, College Park, September 2007. (PhD Thesis).
7. Bohorquez, F.; Samuel, P.; Sirohi, J.; Pines, D.; Rudd, L. & Perel, R. Design, analysis and hover performance of a rotary wing micro air vehicle. *J. Am. Helicopter Society*, 2003, **48**(2), pp. 80–91. doi:10.4050/JAHS.48.80
8. Pereira, J. L. Hover and wind-tunnel testing of shrouded rotors for improved micro air vehicle design. Department of Aerospace Engineering, University of Maryland, College Park, September 2008. (PhD Thesis)
9. Pines, D.J. & Bohorquez, F. Challenges facing future micro air vehicle development. *J. Aircraft*, 2006, **43**(2), 290-305, doi:10.2514/1.4922
10. Hrishikeshvan, V. & Chopra, Inderjit. Aeromechanics and control of a shrouded rotor micro air vehicle in hover and in edgewise flow. *J. Am. Helicopter Society*, 2011, **56**(4), 1-14. doi:10.4050/JAHS.56.042004
11. Singh, P. & Venkatesan, C. Experimental performance evaluation of coaxial rotors for a micro aerial vehicle. *J. Aircraft*, 2013, **50**(5), 1465-1480. doi: 10.2514/1.C031971
12. Hein, B. R. & Chopra, I. Hover performance of a micro air vehicle: Rotors at low reynolds number. *J. Am. Helicopter Society*, 2007, **52**(3), 254-262. doi:10.4050/JAHS.52.254
13. Benedict, M.; Winslow, J.; Hasnain, Z. & Chopra, Inderjit. Experimental investigation of micro air vehicle helicopter rotor in hover. *Int. J. Micro Air Vehicles*, 2015, **7**(3), 231-255. doi:10.1260/1756-8293.7.3.231
14. Ramasamy; Manikandan; Johnson; Bradley & Leishman, J.G. Understanding the aerodynamic efficiency of a hovering micro-rotor. *J. Am. Helicopter Society*, 2008, **53**(4), 412-428.
15. Shrestha, R.; Benedict, M.; Hrishikeshvan, V. & Chopra, Inderjit. Hover performance of a small-scale helicopter rotor for flying on mars. *J. Aircraft*, early edition, 2016, pp. 1160-1167. doi:10.2514/1.C033621
16. Leishman, J.G. Principles of Helicopter Aerodynamics. Cambridge Univ. Press, 2000.

CONTRIBUTORS

Ms Kirti Bhatnagar obtained her BTech (Aeronautical Engineering) from Gautam Buddha Technical University, UP, India. She is working as a Senior Research Associate in the Department of Aerospace Engineering. Her research interests include: Design, analysis and simulation of micro air vehicles.

In the current study, she developed a Blade Element Momentum Theory based micro rotor performance prediction tool and carried out the simulations to understand the effect of rotor geometric parameters on the performance of micro hovering rotor.

Dr Abhishek is an Assistant Professor at the Department of Aerospace Engineering, Indian Institute of Technology Kanpur, India. His research interests include: rotary wing aeromechanics, wind turbines and autonomous unmanned aerial systems with focus on analysis, design and experimentation.

In the current study, he has planned and formulated the research problem and provided guidance in the development of blade element momentum theory simulation. He further, helped in the preparation of the manuscript.